Lasers in Surgery and Medicine 41:305–315 (2009)

ALA-PDT Results in Phenotypic Changes and Decreased Cellular Invasion in Surviving Cancer Cells

Tsuimin Tsai, PHD,[1] Hong Tai Ji, MS,[2] Pei-Chi Chiang, BS,[2] Ruey-Hwang Chou, PhD,[3] Wun-Shaing Wayne Chang, PhD,[3] and Chin-Tin Chen, PhD[2,4]*

[1]*Graduate Institute of Biomedical Materials and Engineering, Graduate School of Dentistry, Taipei Medical University, Taipei 110, Taiwan*

[2]*Institute of Microbiology and Biochemistry, National Taiwan University, Taipei 106, Taiwan*

[3]*Institute of Cancer Research, National Health Research Institutes, Zhunan 350, Taiwan*

[4]*Center for Optoelectronic Biomedicine, National Taiwan University College of Medicine, Taipei 100, Taiwan*

Background and Objectives: The mechanisms of photodynamic therapy (PDT) have been studied on the cellular and tissue levels. However, the cellular behaviors of cancer cells survived from PDT are still not clear. This study attempted to investigate the influence of 5-aminolevulinic acid (ALA)-based PDT on the invasion ability as well as molecular changes in surviving cancer cells and their progeny.

Materials and Methods: The systematic effects of ALA-PDT were evaluated using human invasive carcinoma cells (lung adenocarcinoma CL1-5 cells, melanoma A375 cells and breast carcinoma MDA-MB-231 cells). To study the cellular behaviors of surviving cancer cells, PDT-derived variants were established as stable cell lines after consecutive treatment with ALA-PDT. Scratch wound assay and invasion assay were performed to evaluate the migration and invasion ability in the surviving cancer cells and the established PDT-derived variants. RT-PCR and immunoblot analysis were performed to examine the expression levels of epidermal growth factor receptor (EGFR).

Results: Though ALA-PDT caused differential phototoxicity among these invasive carcinoma cells, reduced migration was found in all the surviving cancer cells Compared to parental cancer cells, the established PDT-derived variants exerted significant phenotypic changes of cellular morphology, reduced mitochondrial function and a suppressed cellular invasiveness. Furthermore, correlated with the reduced invasion ability, expression of EGFR was down-regulated in these established PDT-derived variants.

Conclusions: Except for direct cell killing, ALA-PDT could reduce EGFR expression and invasion ability of the surviving cancer cells and these effects could further pass to the progeny. The results from this study provide insights into a new mechanism by which PDT might affect cellular behaviors and tumor metastasis. Lasers Surg. Med. 41: 305–315, 2009. © 2009 Wiley-Liss, Inc.

Key words: photodynamic therapy; ALA; metastasis; EGF receptor

INTRODUCTION

Photodynamic therapy (PDT), which is based on the uptake of a photosensitizer followed by the selective irradiation of light, is a therapeutic modality for cancer treatment [1–3]. Compared to normal tissues, tumor tissues have higher uptake or retention of photosensitizers that result in the selective destruction of tumor cells after light irradiation. Singlet oxygen is the major cytotoxic agent responsible for the PDT-induced cellular damages [1]. It can only diffuse less than 10 nm during its lifetime and the effective area is estimated less than 5% of the diameter of a typical mammalian cell [4]. Therefore, the subcellular localization of photosensitizer is the major determinant of the primary oxidative damages. Depending on the characteristics of photosensitizer, PDT can damage numerous organelles that cause cytotoxicity in tumor tissues [5]. The cellular responses to PDT depend on the amounts of photosensitizer and the light dose received, which further triggers either cellular repair/recovery or death [5,6]. PDT-induced direct cell killings as well as damage to the exposed microvasculature may cause rapid tumor ablation [3]. In addition to the acute cytotoxic effects, a systemic post-PDT response involving inflammatory changes and subsequent immune response also occurred [7].

Due to the limited light penetration, PDT is generally considered as a local treatment, especially for early carcinoma. Primary tumors are commonly composed of heterogeneous cell populations with different characteristics, such as the metastatic potential [8]. These heterogeneous cells might differ in their ability in photosensitizer uptake or retention, and that influences their sensitivity to PDT or their repairing ability after PDT-induced damage [9]. Considering the limitations of light penetration and

Additional Supporting Information may be found in the online version of this article.

Contract grant sponsor: National Science Council (NSC), Taiwan; Contract grant numbers: 92-2320-B002-094, 93-2320-B002-122; Contract grant sponsor: Department of Health, Taiwan; Contract grant numbers: NHRI-GT-EX89S842C, 94A1-PADOH01.

*Correspondence to: Chin-Tin Chen, PhD, Center for Optoelectronic Biomedicine, National Taiwan University College of Medicine, No 1, Jen-Ai Road, Section 1st, Taipei 100, Taiwan.
E-mail: chintin@ntu.edu.tw

Accepted 19 February 2009
Published online in Wiley InterScience (www.interscience.wiley.com).
DOI 10.1002/lsm.20761

photosensitizer content, certain amounts of tumor cell might recover from PDT-induced damages and survive. Recently, the mechanisms of PDT-induced cytotoxicity have been studied on the cellular and tissue levels [3,5]. However, the cellular behaviors of tumor cells that survived from PDT-induced damage are still not clear. For example, compared with both surgery and no treatment, local PDT of primary tumor results in a decrease in the incidence of distant metastasis [10–12]. It has been suggested that this reduced metastasis relates to the PDT-induced modification of cell adhesion process at the cell surface [13–16]. We recently demonstrated that the increased adherence following ALA-PDT was transient [17]. In this regards, the observed alteration in cell adhesion cannot fully explain the reduction in tumor metastasis after PDT. In addition, using an orthotopic prostate tumor model, Momma et al. [18] showed that PDT gave a significant increase in the mean number of lung metastases. Therefore, it is necessary to further investigate the PDT-induced biological consequences and the cellular behaviors of surviving cancer cells and their progenies.

The aim of this work was to examine the post-PDT response involving its influence on the migration ability as well as molecular changes in surviving cancer cells. The present study shows for the first time that ALA-PDT caused permanently phenotypic morphology alternation, reductions of mitochondrial function and metastatic potential. Furthermore, the downregulation of EGFR and reduced metastatic ability were found in cancer cells that survived from ALA-PDT as well as their progenies.

MATERIALS AND METHODS

Cell Culture and Photodynamic Treatment

CL1-5 cells were derived from a poorly differentiated human lung adenocarcinoma [19] and cultured in RPMI medium containing 10% fetal bovine serum (FBS). Human breast carcinoma MDA-MB-231 was grown in RPMI medium containing 10% FBS. The melanoma A375 cell line was grown in DMEM medium containing 10% FBS. Cells were cultured at 37°C in a humidified atmosphere of 5% CO_2. For ALA-PDT, cells were seeded onto culture dishes or chamber slides and grown overnight in complete medium. Unless specified, cells were then incubated with 1 mM ALA for 3 hours, and then exposed to various doses of light. The light source consisted of high power LED array, with the wavelength centered at 635 ± 5 nm [17]. The fluence rate of LED light source is 60 mW/cm^2. After irradiation, cells were incubated with complete medium until further analysis.

MTT Assay

The MTT [3(4,5-dimethyl-thiazoyl-2-yl)2,5 diphenyl-tetrazolium bromide] assay is based on measuring the activity of mitochondrial dehydrogenases, which can reduce a water-soluble tetrazolium salt to a purple insoluble formazan product. The amount of formazan product was analyzed spectrophotometrically at the absorbance of 570 nm. Cells exposed to ALA but not light were used as control. MTT activity (%) = (mean absorbance of treated cells/mean absorbance of control cells) $\times$ 100%.

Colony-Formation Assay

The PDT-induced phototoxicity was further determined by colongenic assay. Briefly, 1000 cells were seeded into 60-mm dishes. The plating efficiency was higher than 80%. After ALA incubation, cells were exposed to various doses of light. Cells exposed to ALA alone were used as a control. Seven days post ALA-PDT, cells were fixed and stained with 0.5% crystal violet. Colonies containing more than 50 cells were counted. For counting the colony number, a picture of the dish was taken after staining the colony with crystal violet. The picture was then viewed in a computer by using the software of Microsoft Paint. The picture was further divided into 8 areas. Each independent colony was counted one by one in the eight areas of the dish. All experiments were carried out in triplicate.

Determination of Intracellular ALA-Induced PpIX

Exponentially growing cells were seeded at a density of 2×10^5 cells in 60-mm Petri dishes. After incubation with ALA for 3 hours, the medium was removed and cells were trypsinized and resuspended in PBS. The accumulated PpIX content was measured by flow cytometry. A 620-nm band pass filter (605–635 nm) was used to detect the PpIX emission fluorescence under 488-nm argon laser excitation. Fluorescence intensity of the cells was recorded and represents the relative intracellular PpIX content.

Establishment of PDT-Derived Variants

Via consecutive ALA-PDT, CL1-5, A375, and MDA-MB-231 cells were used to obtain variant cells and served as the parental cell lines. To obtain the PDT-derived variants, parental cells plated on 60-mm Petri dishes were incubated with ALA, and then exposed to the various doses of light as indicated. The surviving cells were allowed to proliferate and replated for the following cycle of photosensitization, which takes 3–6 days for each cycle. Survivors of the 1st, 3rd, and 5th cycle were further propagated and established as stable variants for further analysis.

Flow Cytometric Analysis for JC-1 and MTG Analysis

To examine the possible changes of mitochondrial membrane potential and mitochondrial amount in established variants, we stained cell suspensions with 5,5',6,6'-tetrachloro-1,1',3,3'-tetraethylbenzimidazolcarbocyanine iodide (JC-1) and MitoTracker® Green (MTG; Molecular Probes, Eugene, Oregon, USA), respectively [20,21]. Briefly, cells were incubated with MTG (500 nM) or JC-1 (10 μg/ml) for 30 min and analyzed on a cell-by-cell basis under the excitation of 488-nm laser light in a flow cytometry combined with a specific detection system (FACS Calibur™, Becton Dickinson, Franklin Lakes, NJ, USA). The MTG emission fluorescence was collected with a 530 ± 15 nm bandpass filter. For JC-1 analysis, emission signals from red (585 ± 21 nm) and green (530 ± 15 nm) light were isolated by each photomultiplier detector and

processed for digitization 10,000 cells per experiment. The mitochondrial membrane potential was determined by histogram analysis of the ratio of the red to green fluorescence intensities. At least three experiments were performed for each sample cell line.

Determination of Mitochondrial ATP in PDT-Derived Variants

Mitochondrial ATP content of PDT-derived variants was measured with an ATP determination kit according to manufacturer's instructions (Molecular Probes). Briefly, cells were plated and incubated in glucose-free culture medium for 3 hours to avoid the production of ATP via glycolysis. Cells were then lysed with 1% Triton, mixed with ATP reaction buffer and the luminescence was measured by a luminescence counter. The relative luminescence intensities were corrected by the amount of total protein in cell extract. Three measurements were taken for each sample.

Scratch Wound Assay

Cells were seeded into 60-mm dishes at 80% confluence and grown for another 16 hours. Since cell proliferation rates might affect the migration distance, cells were preincubated with 10 μg/ml mitomycin C for 3 hours to block cell division before conducting the migration assays. A denuded area was done by across the diameter of the dish by a rubber policeman. Cells were washed with PBS and further incubated in a complete medium. At the time of 0, 24, 48, and 72 hours post incubation, pictures were taken under microscope at a magnification of 20×. The migration distance at different time point was determined by subtracting the values obtained at hour 0 from 24, 48, or 72 hours.

Invasion Assay

The invasive ability of cells was measured in a trapezoidal modified Boyden chamber [22]. Briefly, a polycarbonate membrane with 10 μm pores coated with Matrigel was placed between the upper- and lower-well plates of a membrane invasion culture system chamber. Subsequently, 5×10^4 cells were seeded onto the upper wells and incubated for 24 hours. Cells invaded through the coated membrane were removed from harvested from the lower wells with 2 mM EDTA, and dot-blotted onto a 0.1% poly-L-lysine coated membrane. After fixation in methanol, blotted cells were stained with 50 μg/ml propidium iodine for 30 min in the dark and the cell number in each blot was counted under a fluorescence microscope at a 25-fold magnification by use of the Analytical Imaging Station software package (Imaging Research, Inc., Saint Catherines, Ontario, Canada).

Immunoblot Analysis

Parental and PDT-derived variant cells were lysed and equal amount of protein lysates were electrophoresed on 10% SDS–polyacrylamide gels. The proteins were transferred to nitrocellulose membrane and reacted with antibodies against EGFR or β-actin (as loading control) (Cell Signaling Technology, Inc., Danvers, MA, USA). Secondary antibody conjugated with horseradish peroxidase was applied and immunocomplex was visualized by Chemiluminescence Reagent Plus (Blossom Biotechnology, Inc., Boston, MA, USA).

Reverse Transcriptase-Polymerase Chain Reaction

Total RNA was extracted from parental or PDT-derived variant cells by using TRIzol reagent (Invitrogen, Carlsbad, CA, USA). An equal amount of RNA of the samples was used to synthesize first-strand cDNA by using SuperScript™ II reverse transcriptase (Invitrogen) according to the manufacturer's instruction. The same cDNA product obtained from each sample was used for subsequent PCR amplification by using Tag DNA polymerase (Invitrogen). Primers used for human EGFR and β-actin (housekeeping gene) are: EGFR (S: 5'-GATAGACG-CAGATAGTCGC-3'; AS: 5'-TTCTTCATCCATCAGGGC-AC-3'); β-actin (S: 5'-TGGACTTCGAGCAAGAGATGG-3'; AS: 5'-ATCTCCTTCTGCATCC-TGTCG-3'), respectively. The PCR product was then analyzed by electrophoresis on 2% agarose gels. Densitometric analyses of the PCR products were analyzed by using the UVP LabWork Software 4.6. The mRNA ratio between EGFR and β-actin was calculated to normalize for initial variations in sample concentration.

Statistical Analysis

All experiments were repeated at least three times with 4–6 parallel measurements in different dishes or slides. Results were averaged for experiments performed under similar conditions and expressed as the mean ± SD. unless stated otherwise. The statistical significance of differences in the results was analyzed using Student's *t*-test for paired data or one-way ANOVA test for multiple comparisons. A value of $P<0.05$ was accepted as statistically significant.

RESULTS

Differential Phototoxicity Relates to the Different PpIX Contents in Cancer Cells With Invasiveness

To analyze the phototoxicity induced by ALA-PDT in the invasive cancer cells, lung adenocarcinoma CL1-5 cells, breast carcinoma MDA-MB-231cells, and melanoma A375 cells were used. These cell lines were derived from different human cancerous tissues. The cellular survival was estimated by MTT assay at 24 hours after light irradiation. Cells incubated with ALA alone showed a 100% survival. ALA-PDT-induced cancer cell deaths were significantly found in A375 and MDA-MB-231 invasive cancer cells and increased in a light-dose dependent manner (Fig. 1A). The 50% lethal light dose (LD_{50}) for A375 and MDA-MB-231 cells are around 3 and 2 J/cm^2, respectively. However, less than 20% of cell death was found in CL1-5 cells even the light dose was increased up to 18 J/cm^2. However, the survival rate of CL1-5 cells was not decreased even the ALA concentrations were increased (data not shown).

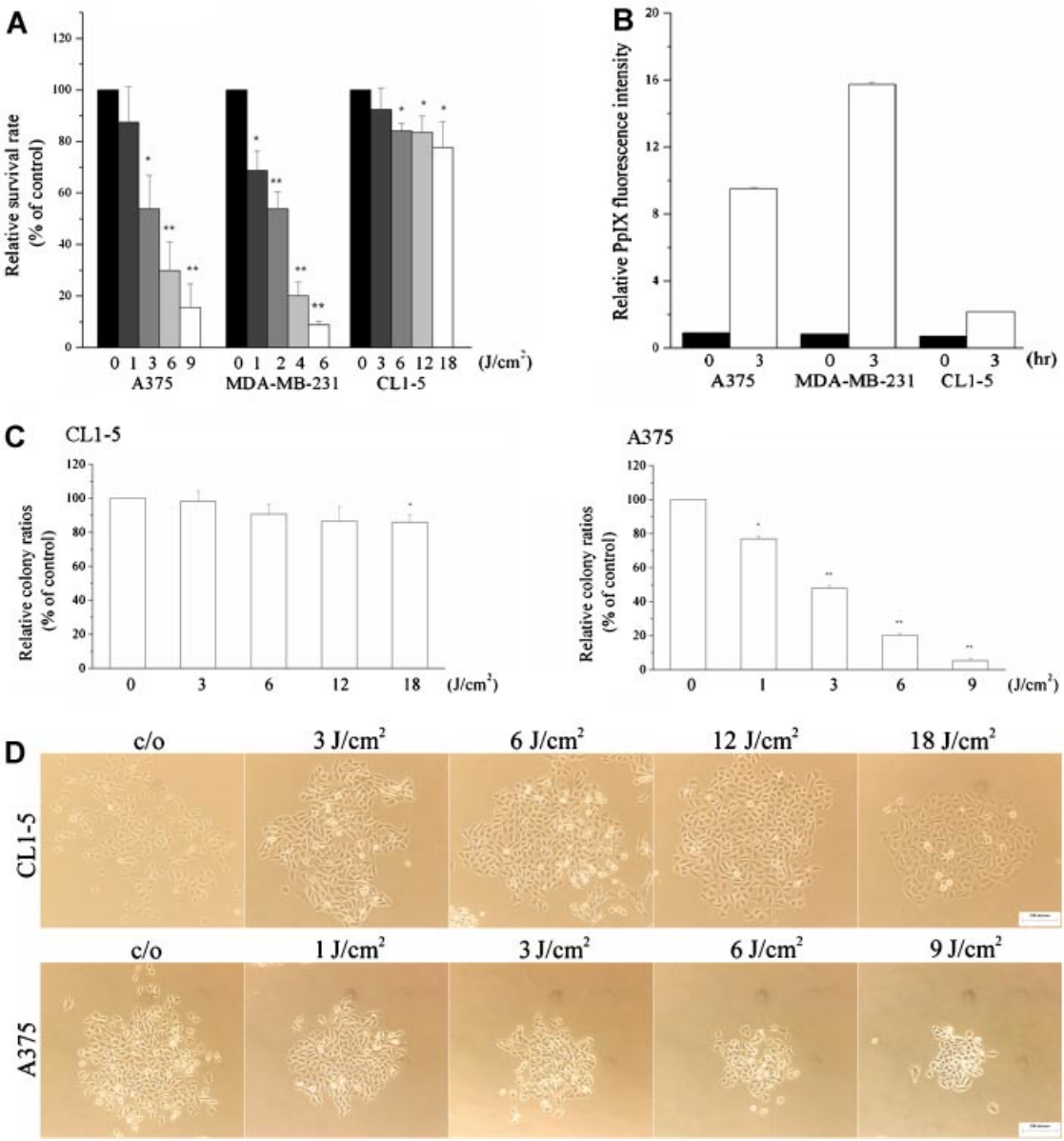

Fig. 1. ALA-PDT induced differential phototoxicity in invasive cancer cells. **A**: Cell viability was determined by MTT assay at 24 hours after light irradiation. Cells exposed to ALA only were used as a control and shown as 100% survival rate. Points represent the average values from three experiments and expressed as mean ± SD. **B**: After 3-hr incubation of 1 mM ALA, the PpIX content was measured by flow cytometry. Each point represented the relative mean ± SD obtained from three independent experiments. **C**: Clonogenic assay was further performed to examine the cell viability of CL1-5 and A375. Colonies containing more than 50 cells were counted at 7 days post ALA-PDT. Cells exposed to ALA only were used as a control and represented a 100% survival. **D**: In response to ALA-PDT, CL1-5, and A375 cells formed compact colonies. The colonies become more condense when the light dose increased.

Since the amount of ALA-converted PpIX might affect phototoxicity, we further examined whether the differential cytotoxicity was due to the different PpIX contents in cancer cells. Compared to other cancer cell lines, PpIX accumulation was very low in CL1-5 cells (Fig. 1B) and was not changed significantly as the ALA concentrations were increased (data not shown). The low PpIX content in CL1-5 cells explains the relative low phototoxicity to ALA-PDT. Meanwhile, the relative high PpIX content in MDA-MB-231 cells explains its high phototoxicity after light irradiation. These results indicated the differential phototoxicity among these three cell lines might be due to the differential ALA-converted PpIX content.

To avoid misinterpretation of the overall death using MTT assay, clonogenic assay was performed to further

assess the proliferation ability of CL1-5 and A375 after ALA-PDT. As illustrated in Figure 1C, the ALA-PDT-induced cytotoxicity of A375 cells was significantly increased in a light-dose dependent manner with LD_{50} around 3 J/cm^2. The typical colony images of control and LD_{50} was shown in supplementary 1. Meanwhile, clonogenic survival rate also showed the relative low phototoxicity to ALA-PDT in CL1-5 cells, which still showed an over 85% of survival rate even the light dose was increased up to 18 J/cm^2. Noted that, although there is differential cytotoxicity among these cancer cells, all the PDT-treated cells formed dense colonies and the colonies got more condense when the light dose was increased (Fig. 1D).

Reduced Migration Ability in PDT-Treated Cells

The more condense colony formed after ALA-PDT suggests that the migration ability of cancer cells survived from ALA-PDT might be affected. To examine this possibility, we first treated CL1-5, A375, and MDA-MB-231 cancer cells with ALA-PDT under the light dose of 6, 3, and 1 J/cm^2, respectively. After ALA-PDT, the survived cells were kept for further growth. Then, the migration rate was measured using scratch wound assay. As shown in Figure 2, a significant reduction in migration was found in CL1-5, A375, and MDA-MB-231 cancer cells survived from ALA-PDT. These results suggest that the photodamage induced by ALA-PDT caused the suppression of cell migration ability. It should be noted here that the reduced migration rate was not related to the level of phototoxicity because CL1-5 cells showing insensitive to ALA-PDT had significant reduction in cell migration as found in A375 and MDA-MB-231 cells.

ALA-PDT Results in Mitochondrial Damage and Phenotypic Change

As shown above, reduced migration rate was found in cancer cells survived from ALA-PDT. Whether this reduced migration is a transient or permanent PDT-induced photodamage deserves further investigation. To study the cellular behaviors of surviving cancer cells and their progeny, we established stable PDT-derived variants by having cancer cells under multiple treatments with ALA-PDT. In these experiments, CL1-5, A375, and MDA-MB-231 cells were treated with consecutive cycles of ALA-PDT under various light doses. Surviving cells were then cultured in complete medium and further established as stable clones. The established PDT-derived variants designed as CL1-5/3A5 and CL1-5/6A5 was treated with ALA-PDT at a light dose of 3 and 6 J/cm^2 for five cycles, respectively. Similarly, the A375 and MDA-MB-231 variants were established and maintained as stable cell lines, which were designed as A375/3A5 and MDA-MB-231/1A5 after five consecutive cycles of ALA-PDT at 3 and 1 J/cm^2, respectively. Interestingly, the established CL1-5/6A5, A375/3A5, and MDA-MB-231/1A5 variants have permanent morphological changes. Compared to the fibroblastic morphology of parental cells, they all showed polygonal

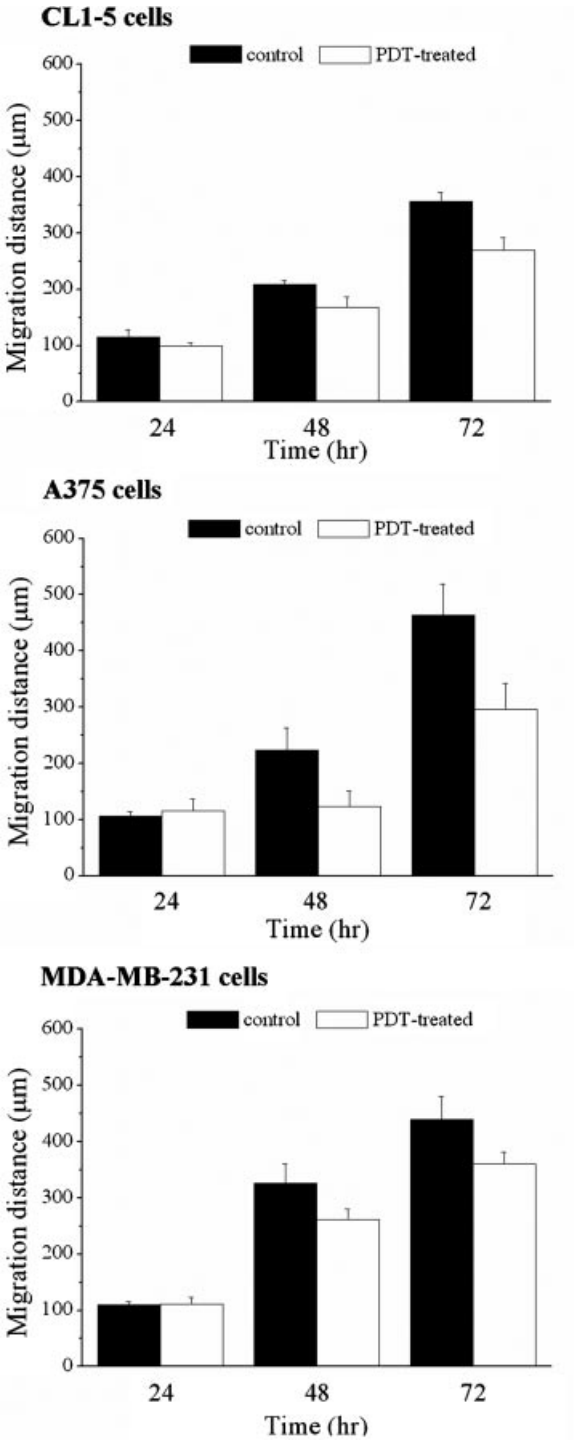

Fig. 2. Cancer cells survived ALA-PDT had reduced migration ability. CL1-5, A375, and MDA-MB-231 cells were treated with ALA-PDT under the light dose of 6, 3, and 1 J/cm^2, respectively. After ALA-PDT, surviving cells were allowed to proliferate and then replate. Cells exposed to ALA only were used as a control. By using scratch wound assay, the migration distance at different time point was determined by subtracting the values obtained at hour 0 from 24, 48, or 72 hours. The migration distance (μm) was measured at the time indicated.

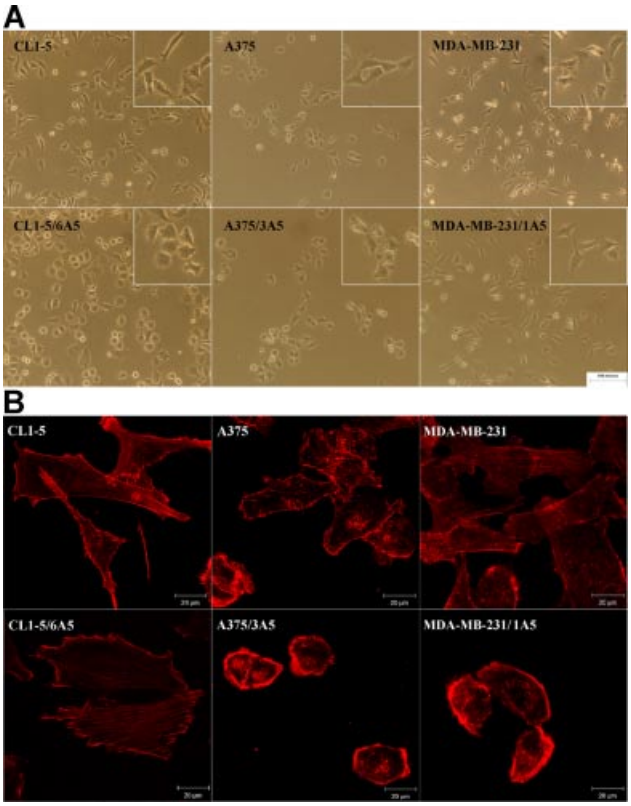

Fig. 3. ALA-PDT derived variant cells maintain a polygonal cell morphology. **A**: Compared to parental cells (**upper panel**), phase-contrast images (magnification 200×) show significant morphological alterations in ALA-PDT derived variants (**lower panel**) under microscope. The insets show higher magnifications 400×. **B**: Parental and PDT-derived variant cells were stained with 0.1 μM of Rhodamine Phalloidin (Molecular Probes) to visualize the actin stress fiber and examined under confocal microscope.

morphology (Fig. 3A). In addition, the F-actin was re-organized from the longitudinal stress fibers to the cell-substrate interface with a rim of cortical actin, which suggests the increased adherence to the substratum (Fig. 3B).

Previously, we have shown that ALA-PDT could cause mitochondria dysfunction [17]. Therefore, we further examined the integrity of mitochondria in the established PDT-derived variants. As shown in Table 1, compared to parental cells, the mitochondrial membrane potential evaluated by JC-1 was significantly reduced in CL1-5/6A5, A375/3A5, and MDA-MB-231/1A5 variants. The levels of mitochondrial ATP in PDT-derived variants were also reduced (Table 1). However, there was no significant difference in the mitochondrial content between the parental and PDT-derived variants as judged by the MTG fluorescence intensity. Collectively, these results clearly showed that consecutive ALA-PDT caused permanent mitochondrial damage in the established PDT-derived variants.

PDT-Derived Variants Are not PDT-Resistant Cells but Exhibit Reduced Migration and Invasiveness

As these PDT-derived variants were established from cells that survived from five consecutive cycles of ALA-PDT, it is reasonable to suspect that these variants might be resistant to ALA-PDT. To address this issue, we further compared the phototoxicity induced by ALA-PDT between the parental cells and PDT-derived variants. Although PDT-derived variants showed higher cell proliferation rate (Supplementary 2), our studies showed that ALA-PDT did not cause significant difference in phototoxicity between parental cells and PDT-derived variants (Supplementary 3). These results suggest that these PDT-derived variants are not resistant to ALA-PDT.

We then examined whether the migration ability was permanently affected in the established PDT-derived variants by scratch wound assay. As illustrated in Figure 4A, compared to parental CL1-5 cells, PDT-derived CL1-5 variants showed a significant reduction in migration rate, which was correlated with the treatment cycles and light dose. Similar phenomena were also found in PDT-derived A375 and MDA-MB-231 variants (Fig. 4B). As motility is a key factor in regulating cancer cell invasion [23], we further examined whether this inhibition affected the metastatic potential in ALA-PDT-derived variants by examining the transmigration of a Matrigel barrier. Invasion chamber analysis demonstrated that, compared to CL1-5 cells (100%), the invasion rate of CL1-5/6A1, CL1-5/6A3, and CL1-5/6A5 variants were $64.9 \pm 19.2\%$, $38.9 \pm 5.9\%$, and $25.0 \pm 8.1\%$, respectively. The invasion rate of CL1-5/3A5 and CL1-5/6A5 were $49.0 \pm 27.8\%$ and $21.4 \pm 13.3\%$, respectively (Fig. 4C). The generality of the sustained ALA-PDT effect on cellular invasiveness was also found in the PDT-derived variants of A375 and MDA-MB-231. The invasiveness was reduced to 65.2% and 68.9% in A375/3A5 and MDA-MB-231/1A5 variants, respectively (Table 1). These results indicate that cancer cells that survived ALA-PDT were damaged in mitochondria and showed a reduction in cell migration and invasiveness.

The Reduction of EGF Receptor in PDT-Derived Variants

Overexpression of EGFR is found in different types of human tumors and often correlates with the enhanced cellular proliferation and development of cancer metastasis [24,25]. Moreover, down-regulation of EGFR has been noted in PDT-treated cells in vitro and in vivo [26]. We therefore investigated whether the decreased cell migration and invasiveness in PDT-derived variants are related to the downregulation of EGFR. As shown in Figure 5A, compared to parental CL1-5 cells, ALA-PDT caused a reduction in the mRNA level of EGFR, which was proportional to the treatment cycles and light dose. Similarly, the reduced EGFR was also found in PDT-derived A375 and MDA-MB-231 variants (Fig. 5B). Meanwhile, immunoblotting analysis further showed ALA-PDT results in a significant decrease of the EGFR protein levels in these PDT-derived variants (Fig. 6). These results suggest

TABLE 1. Relationship Between the Mitochondrial Function and Cellular Invasion Ability in Parental and Established PDT-Derived Variant Cells

Cell line[a]	Mitochondrial content (cps[c])	Mitochondrial function: JC-1 membrane potential (%)	Mitochondrial function: ATP content (arbitrary U/μg)	Relative invasion ability (%)
CL1-5				
Parental	34.6 ± 3.8	0.88 ± 0.04	0.85 ± 0.07	100
6A5	37.1 ± 1.0	0.78 ± 0.01[b]	0.34 ± 0.07[b]	21.4 ± 13.3[b]
A375				
Parental	28.1 ± 0.8	1.50 ± 0.04	0.13 ± 0.01	100
3A5	25.6 ± 2.4	1.19 ± 0.03[b]	0.07 ± 0.01[b]	65.2 ± 14.6[b]
MDA-MB-231				
Parental	51.4 ± 4.8	3.91 ± 0.43	0.32 ± 0.03	100
1A5	60.7 ± 15.1	2.83 ± 0.19[b]	0.23 ± 0.03[b]	68.9 ± 17.5[b]

[a]CL1-5/6A5, A375/3A5, and MDA-MB-231/1A5 were established with consecutive five cycles of ALA-PDT under the light dose of 6, 3, and 1 J/cm^2, respectively.
[b]$P < 0.05$ for difference between parental and PDT-derived variants.
[c]CPS is the unit of fluorescence intensity of MitoTracker Green measured by flow cytometry which is used to express the relative mitochondrial content per cell.

that the consecutive treatment of ALA-PDT results in the down-regulation of EGFR, which correlates with the reduced migration and invasion in the PDT-derived variants.

DISCUSSION

In this study, we used cancer cell lines derived from different human carcinomas to examine the phototoxicity and subsequent biological effects of invasive cells that survived from ALA-PDT. Tumor cells are known to accumulate more PpIX, which makes ALA successful in diagnosis and treatment for tumor tissues [27]. This might attribute to the aberration of heme biosynthesis, such as the reduction of ferrochelatase (FC) activity or the increase of porphobilinogen deaminase (PBGD) activity within the tumor cells [28,29]. However, this study showed that CL1-5 cells derived from human lung adenocarcinoma responded poorly to ALA-PDT due to the lower amounts of ALA-converted PpIX (Fig. 1). Whether CL1-5 cells have aberrant PBGD or FC activity, which might be contradictory to the known roles of PBGD or FC in tumor cells, deserves further investigation. In addition, it should be noted that the poor response of CL1-5 cells did not reflect a general resistance of lung adenocarcinoma to ALA-PDT because significant phototoxicity was found in the other lung adenocarcinoma H1299 cell line (data not shown). In fact, this study clearly indicates that different cancer cells might respond differentially to PDT. In this regards, it is important to study the biological consequences and molecular changes of surviving cancer cells after PDT.

One of the major findings in this study is that ALA-PDT-induced photodamage impairs the migration ability in cancer cells. This effect caused by ALA-DPT could pass to their progeny. This was supported by the following evidences. First, after ALA-PDT, the surviving cancer cells form more dense colonies with less space between cells (Fig. 1D). It should be noted that the progeny of surviving cancer cells did not receive ALA-PDT but their forming colonies are more compact. Second, the reduced migration was further verified by wounding the confluent monolayer of CL1-5, A375, and MDA-MB-231 cancer cells survived from ALA-PDT (Fig. 2). Finally, compared to those of the parental cells, the established PDT-derived variants showed not only reduced migration but also reduced invasion in Matrigel (Fig. 4). It has been accepted that there are clonal variations with heterogeneous characteristics in established cell lines. It is possible that some of the clones in parental cells used in this study might have similar morphology and migration ability as found in the PDT-derived variants. Although our present studies indicate that the PDT-derived variants are due to the PDT selection process, it would be better to further investigate the differences between the PDT-derived variants and clones of parental cells with similar phenotype. In the future, pure clones from parental cells and PDT-derived variants with similar morphological phenotype will be helpful in addressing this issue.

PDT-induced suppression of tumor metastasis has been reported, which was mainly ascribed to direct cell killing and microvascular destruction of tumor [11–13]. In addition, this reduced metastatic potential is also linked to the direct impairment of adhesion molecules at the plasma membrane [15,30] or indirect deterioration of cell adhesion [16,31]. In fact, following ALA-PDT, all the cancer cells used in this study also showed transient morphological alterations and increased adherence as previously found in NIH3T3 cells [17]. However, this increased adherence is transient and is not found in PDT-derived variants (data not shown). Therefore, the reduced invasion of PDT-derived variants might not fully be related to the PDT-induced immediate deterioration of cell adhesion.

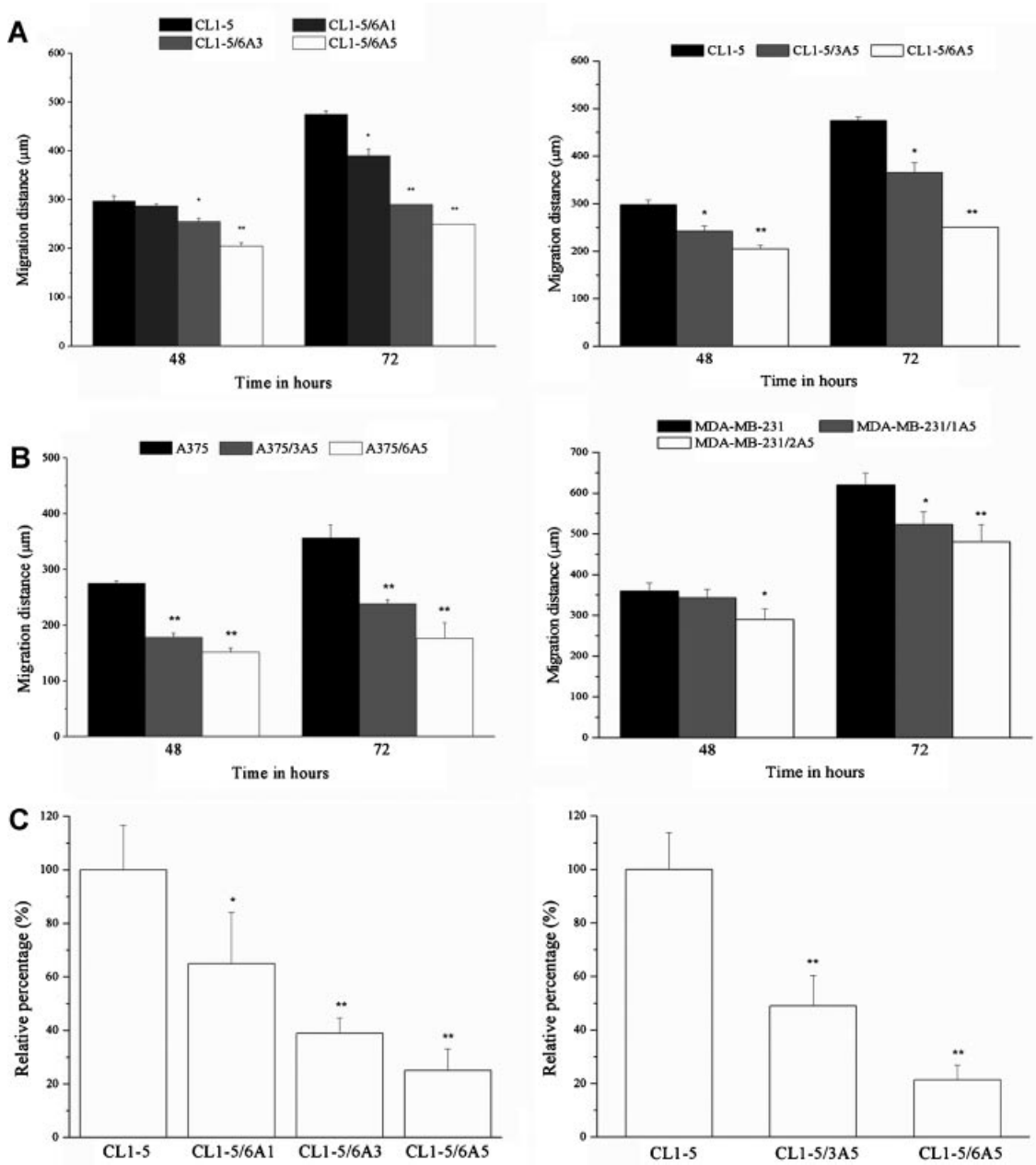

Fig. 4. ALA-PDT derived variants show reduced migration and invasion ability. **A**: By using scratch wound assay, the migration distance at different time point was determined by subtracting the values obtained at hour 0 from 48 or 72 hours. The migration distance (μm) was measured at the time indicated. Compared to parental CL1-5 cells, PDT-derived CL1-5 variant cells showed reduced migration ability in a treatment-cycle (**left panel**) and light-dose (**right panel**) dependent manner. **B**: Similar results of migration ability were found in the PDT-derived variants of A375 and MDA-MB-231. **C**: The Matrigel invasion assays demonstrated the values of relative invasiveness of PDT-derived variants normalized with those of parental CL1-5 (100%). PDT-derived CL1-5 variants showed a significant decrease of invasiveness, which was corrected with the treatment cycles (**left panel**) and light dose (**right panel**). These results are the average of three independent experiments and expressed as mean ± SD. $^{*}P<0.05$; $^{**}P<0.01$ statistically significant difference compared with the parental cells.

Recently, Casas et al. [32,33] have shown that cells resistant to ALA-PDT have disorganized cytoskeleton and decreased metastatic phenotype. Although the established PDT-derived variants of this study were not PDT resistant (Supplementary 3), they still showed reduced ability in the migration and invasion. These results suggest that PDT-induced photodamage could decrease the metastatic potential in surviving cancer cells. Furthermore, our finding in

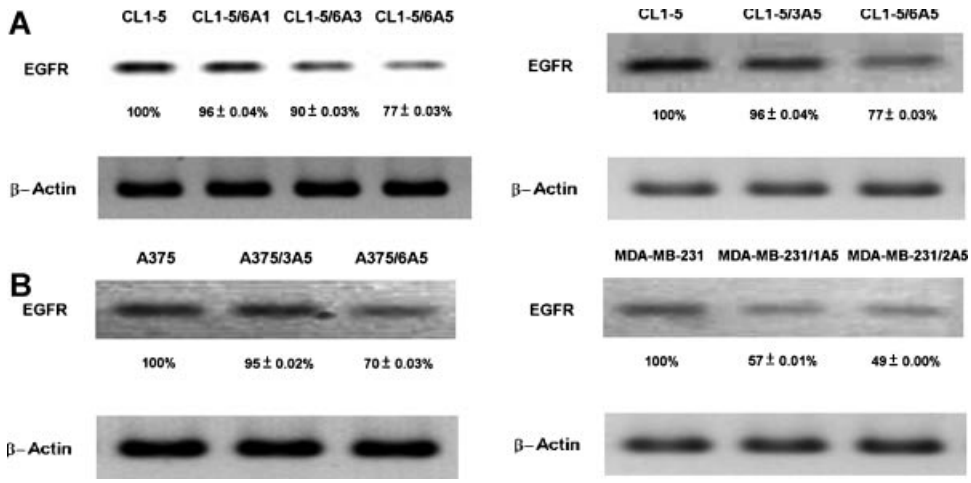

Fig. 5. ALA-PDT results in the down-regulation of EGFR mRNA in a treatment-cycle and light-dose dependent manner. **A**: CL1-5 cells were treated with various cycles of ALA-PDT (6 J/cm^2; **left panel**) or under various light doses for five consecutive cycles of ALA-PDT (3 and 6 J/cm^2; **right panel**). **B**: The reduction of EGFR mRNA was also found in the PDT-derived variants of A375 and MDA-MB-231. The mRNA levels of β-actin served as a loading control.

the decreased EGFR expression of PDT-derived variants might provide an alternative explanation for the reduced invasion. Down-regulation of EGFR in PDT-treated cells has been linked to antiproliferative effects of PDT [26] or immediate loss of cellular response to growth factor, which could be recovered in post-PDT cells [34]. In this study, we found that the reduced migration correlates with the down-regulation of EGFR. It is important to emphasize here that the reduced EGFR and invasive behaviors were irreversible even the established PDT-derived variants were cultured in normal medium for over 30 growth cycles. These results indicate that ALA-PDT might affect the cancer cell behaviors, such as the reduction of EGFR levels and invasion ability in the surviving cancer cells, which could be passed to their progeny. These findings might further explain why PDT can suppress the tumor metastasis as reported in animal study [11,12,15,16]. It is important to further verify these observations in an in vivo setting by using cancer cell lines with spontaneous metastasis, because the cell lines used in this study can only grow as primary tumors after subcutaneous injection.

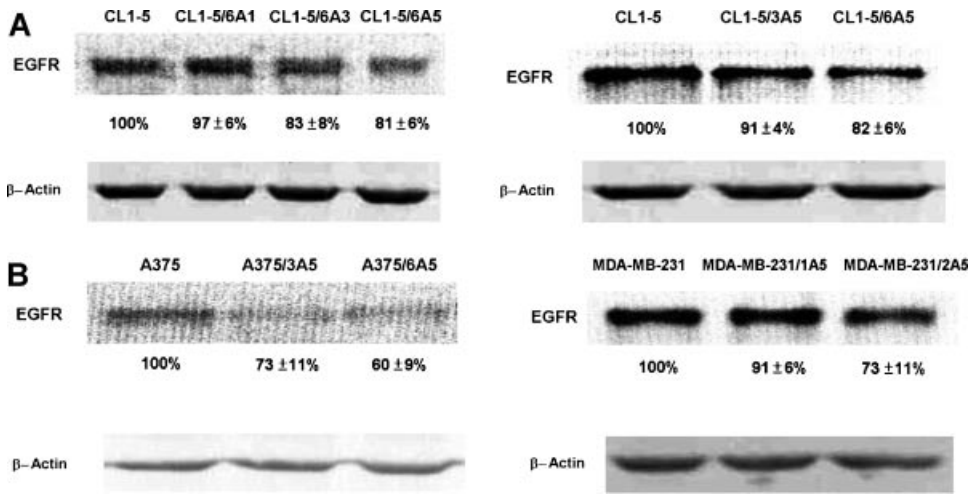

Fig. 6. ALA-PDT results in the down-regulation of EGFR protein levels in a treatment-cycle and light-dose dependent manner. **A**: CL1-5 cells were treated with various cycles of ALA-PDT (6 J/cm^2; **left panel**) or under different light dose for five cycles of ALA-PDT (3 and 6 J/cm^2; **right panel**). The cell lysates were subjected to SDS–PAGE and analyzed by immunoblotting. The levels of β-actin served as a loading control. Compared to parental CL1-5 cells, PDT-derived CL1-5 variant cells have reduced EGFR protein determined. **B**: The reduced expression of EGFR protein was also found in the PDT-derived variants of A375 and MDA-MB-231.

The changes of phenotype and invasion ability usually involve expression changes at the level of nuclear genes. Due to the short diffusion distance of singlet oxygen, the sites of direct photodamage could be correlated to the sites of photosensitizer location [35]. Under our experimental conditions, PpIX was mainly localized at mitochondria as evidenced by the superimposed images of PpIX and MTG in CL1-5 cells (Supplementary 4). Electron microscopic analysis demonstrated that the mitochondria showed a larger size and contained fewer cistae after ALA-PDT (Supplementary 5), indicating mitochondrial swelling. In this regard, it is unlikely that this mitochondria-based PDT will directly damage the nuclear DNA. One possible explanation to the reduced invasion ability in PDT-derived variants is the dissipation of mitochondrial membrane potential (Table 1). It is possible that the abnormal mitochondria somehow gradually alter the nuclear gene expression profile and thus morphological phenotypes and invasiveness. The cytosolic Ca^{2+} has been proposed as the possible link between abnormal mitochondria and the changes of nuclear gene expression [36]. The elevation of cytosolic Ca^{2+} levels could influence several signaling cascades regulating cell adhesion and metastasis [37,38]. Compared to parental cancer cells, we did observe a significant increase of cytosolic Ca^{2+} level in PDT-derived variants (unpublished results). Therefore, it is worthwhile to further investigate whether the cytosolic [Ca^{2+}] plays a critical role in affecting the nuclear gene expression, and that further results in the alterations of cellular morphology and invasiveness in the PDT-derived variants of cancer cells.

In conclusion, we have found that cancer cells survived from ALA-PDT have permanent morphological change and reduced metastatic potential. Further studies are needed to investigate the molecular mechanisms underlying the induction of phenotypic changes and the decrease of cellular invasion ability in the PDT-derived variant cells. Understanding this mechanistic basis and molecular changes can portray a more complete picture of why cancer cells that survived PDT have reduced metastatic ability and therefore are of great significance in PDT biology.

ACKNOWLEDGMENTS

The authors thank Dr. Sung-Tsang Hsieh for assistance on the electron microscopic experiment, Dr. Wen-Sen Lee at Taipei Medical University for the fruitful discussions and Dr. Steven Estus at University of Kentucky for critical reading of the manuscript. We thank the staff of the Second Core Lab, Department of Medical Research, National Taiwan University for technique support during this study.

REFERENCES

1. Gomer CJ, Rucker N, Ferrario A, Wong S. Properties and applications of photodynamic therapy. Radiat Res 1989;120: 1–18.
2. Dougherty TJ, Gomer CJ, Henderson BW, Jori G, Kessel D, Korbelik M, Moan J, Peng Q. Photodynamic therapy. J Natl Cancer Inst 1998;90:889–905.
3. Dolmans DE, Fukumura D, Jain RK. Photodynamic therapy for cancer. Nat Rev Cancer 2003;3:380–387.
4. Moan J, Berg K. The photodegradation of porphyrins in cells can be used to estimate the lifetime of singlet oxygen. Photochem Photobiol 1991;53:549–553.
5. Oleinick NL, Evans HH. The photobiology and photodynamic therapy: Cellular targets and mechanisms. Radiat Res 1998; 150:S146–S156.
6. Kessel D, Luo Y, Deng Y, Chang CK. The role of subcellular localization in initiation of apoptosis by photodynamic therapy. Photochem Photobiol 1997;65:422–426.
7. Castano AP, Morz P, Hamblin MR. Photodynamic therapy and anti-tumor immunity. Nature Rev Cancer 2006;6:535–545.
8. Heppner GH. Tumor heterogeneity. Cancer Res 1984;44: 2259–2265.
9. Rousset N, Vonarx V, Eleouet S, Carre J, Bourre L, Lajat Y, Patrice T. Cellular distribution and phototoxicity of Benzoporphyrin derivative and Photofrin. Res Exp Med 2000;199: 341–357.
10. Canti G, Lattuada D, Nicolin A, Taroni P, Valentini G, Cubeddu R. Antitumor immunity induced by photodynamic therapy with aluminum disulfonated phthalocyanines and laser light. Anticancer Drugs 1994;5:443–447.
11. Gomer CJ, Ferrario A, Murphee AL. The effect of localized porphyrin photodynamic therapy on the induction of tumor metastasis. Br J Cancer 1987;56:27–32.
12. Schreiber S, Gross S, Brandis A, Harmelin A, Rosenbach-Belkin V, Scherz A, Salomon Y. Local photodynamic therapy (PDT) of rat C6 glioma xenografts with Pd-bacteriopheophorbide leads to decreased metastasis and increase of animal cure compared with surgery. Int J Cancer 2002;99:279–285.
13. Denstman SC, Dillehay LE, Williams JR. Enhanced susceptibility to HPD-sensitized phototoxicity and correlated resistance to trypsin detachment in SV40 transformed IMR-90 cells. Photochem Photobiol 1986;43:145–147.
14. Foultier MT, Vonarx-Coinsmann V, Cordel S, Combre A, Patrice T. Modulation of colonic cancer cell adhesiveness by haematoporphyrin derivative photodynamic therapy. J Photochem Photobiol B Biol 1994;23:9–17.
15. Rousset N, Vonarx V, Eleouet S, Carre J, Kerninon E, Lajat Y, Patrice T. Effects of photodynamic therapy on adhesion molecules and metastasis. J Photochem Photobiol B Biol 1999;52:65–73.
16. Uzdensky A, Juzeniene A, Ma LW, Moan J. Photodynamic inhibition of enzymatic detachment of human cancer cells from a substratum. Biochim Biophys Acta 2004;1670:1–11.
17. Tsai JC, Wu CL, Chien HF, Chen CT. Reorganization of cytoskeleton induced by 5-aminolevulinic acid-mediated photodynamic therapy and its correlation with mitochondrial dysfunction. Lasers Surg Med 2005;36:398–408.
18. Momma T, Hamblin MR, Wu HC, Hasan T. Photodynamic therapy of orthotopic prostate cancer with benzoporphyrin derivative: Local control and distant metastasis. Can Res 1998;58:5425–5431.
19. Chu YW, Yang PC, Yang SC, Shyu YC, Hendrix MJ, Wu R, Wu CW. Selection of invasive and metastatic subpopulations from a human lung adenocarcinoma cell line. Am J Respir Cell Mol Biol 1997;17:353–360.
20. Smiley ST, Reers M, Mottola-Hartshom C, Lin M, Chen A, Smith TW, Steele GD, Jr., Chen LB. Intracellular heterogeneity in mitochondrial membrane potentials revealed by a J-aggregate-forming lipophilic cation JC-1. Proc Natl Acad Sci USA 1991;88:3671–3675.
21. Mancini M, Anderson BJ, Caldwell E, Sadghinasab M, Paty PB, Hockenbery DM. Mitochondrial proliferation and paradoxical membrane depolarization during terminal differentiation and apoptosis in a human colon carcinoma cell line. J Cell Biol 1997;138:449–469.
22. Chou RH, Lin KC, Lin SC, Cheng JY, Wu CW, Chang WS. Cost-effective trapezoidal modified Boyden chamber with comparable accuracy to a commercial apparatus. Biotechniques 2004;37:724–726.
23. Wells A. Tumor invasion: Role of growth factor-induced cell motility. Adv Cancer Res 2000;78:31–101.

24. Spaulding DC, Spaulding BO. Epidermal growth factor receptor expression and measurement in solid tumors. Semin Oncol 2002;29:45–54.
25. Herbst RS. Review of epidermal growth factor receptor biology. Int J Rad Oncol Phys 2004;59:21–26.
26. Ahmad N, Kalka K, Mukhtar H. In vitro and in vivo inhibition of epidermal growth factor receptor-tyrosine kinase pathway by photodynamic therapy. Oncogene 2001; 20:2314–2317.
27. Peng Q, Berg K, Moan J, Kongshaug M, Nesland JM. 5-Aminolevulinic acid-based photodynamic therapy: Principles and experimental research. Photochem Photobiol 1997;65: 235–251.
28. Dailey HA, Smith A. Differential interaction of porphyrins used in photoradiation therapy with ferrochelatase. Biochem J 1984;223:441–445.
29. Gibson SL, Cupriks DJ, Havens JJ, Nguyen ML, Hilf R. A regulatory role for porphobilinogen deaminase (PBGD) in δ-aminolevulinic acid-induced photosensitization? Br J Cancer 1998;77:235–243.
30. Runnels JM, Chen N, Ortel B, Kato D, Hasan T. BPD-MA-mediated photosensitization in vitro and in vivo: Cellular adhesion and β1 integrin expression in ovarian cancer cells. Br J Cancer 1990;80:946–953.
31. Uzdensky A, Kolpakova E, Juzeniene A, Juzenas P, Moan J. The effect of sub-lethal ALA-PDT on the cytoskeleton and adhesion of cultured human cancer cells. Biochim Biophys Acta 2005;1722:43–50.
32. Casas A, Sanz-Rodriguez F, Di Venosa G, Rodriguez L, Mamone L, Blazquez A, Jaen P, Batlle A, Stockert JC, Juarranz A. Disorganization of cytoskeleton in cells resistant to photodynamic treatment with decreased metastatic phenotype. Cancer Lett 2008;270:56–65.
33. Casas A, Di Venosa G, Vanzulli S, Perotti C, Mamone L, Rodriguez L, Simian M, Juarranz A, Pontiggia O, Hasan T, Batlle A. Decreased metastatic phenotype in cells resistant to aminolevulinic acid-photodynamic therapy. Cancer Lett 2008;271:342–351.
34. Wong T-W, Tracy E, Oseroff AR, Baumann H. Photodynamic therapy mediates immediate loss of cellular responsiveness to cytokines and growth factors. Cancer Res 2003;63:3812–3818.
35. Peng Q, Moan J, Nesland JM. Correlation of subcellular and intratumoral photosensitizer localization with ultrastructural features after photodynamic therapy. Ultrastruct Pathol 1996;20:109–129.
36. Butow RA, Avadhani NG. Mitochondrial signaling: The retrograde response. Mol Cell 2004;14:1–15.
37. Berridge MJ, Lipp P, Bootman MD. The versatility and universality of calcium signaling. Nat Rev Mol Cell Biol 2000; 1:11–21.
38. Amuthan G, Biswas G, Ananadatheerthavarada HK, Vijayasarathy C, Shephard HM, Avadhani NG. Mitochondrial stress induced calcium signaling, phenotypic changes and invasive behavior in human lung carcinoma A549 cells. Oncogene 2002;21:7839–7849.